JOURNAL OF MATERIALS SCIENCE 21 (1986) 314–320

Dynamic studies of peel failure in metallized polyester films

D. J. BROWN*, A. H. WINDLE
Department of Metallurgy and Materials Science, University of Cambridge, Pembroke Street, Cambridge CB2 3QZ, UK

D. G. GILBERT‡, P. W. R. BEAUMONT
Department of Engineering, University of Cambridge, Trumpington Street, Cambridge CB2 1PZ, UK

Peel failure in PET–aluminium–PET laminates has been studied by dynamic scanning electron microscopy (SEM). The mechanisms of failure are identified, and dynamic observations correlated with conventional SEM fractography. Plastic deformation is highly localized in a region several microns thick. In well-bonded regions the "peel crack" propagates by an advance microcracking mechanism, allowing changes of fracture plane which are accompanied by the formation, extension and breakage of ligaments drawn out from the surface layers of PET. The origin of localized deformation and possible factors affecting the locus of failure are dicussed.

1. Introduction

Commercial and technological applications of polymer films frequently require a high level of resistance to mechanical handling and stress. In particular, the widespread use of composite films produced by lamination demands that high laminate failure strengths be achieved. It is thus necessary first to create a strong interface – sufficiently strong to ensure that when failure does occur it proceeds by a cohesive route within the polymer rather than an interfacial one – and then to ensure that the energy associated with the cohesive failure is maximized. In service, failure of a laminate will often occur in some form of peeling situation. This process may be likened to the propagation of a crack along or near the interface, so that one is concerned with the mechanisms of energy dissipation in the vicinity of an advancing "peel crack": that is, with making the peel crack propagation as expensive (in energy terms) as possible.

This paper concerns the mechanisms of peel failure in laminates constructed from biaxially drawn poly(ethylene terephthalate) (PET) films. Two such films are bonded together under pressure using the method developed by Gibbins and Windle [1], in which a thermally evaporated layer of aluminium is deposited on to the surfaces as they are brought together in a vacuum chamber, thus forming a polymer–metal–polymer laminate with the central metal layer some tens of nanometres in thickness. The high peel strengths (several hundred Jm^{-2}) attainable in these laminates are associated with failure paths which deviate well away from the metal layer and "probe" into the bulk properties of the polyester films. In investigating the attainment of such high peel strengths in a metal–polymer system, the symmetrical "sandwich" geometry offers a major advantage over earlier techniques involving the pull-off of a glued stud or of a strip of proprietary adhesive tape. The latter methods will only produce failure of the specimen when the strength is low or moderate, and even then the measured failure energy owes more to deformation of the glue on the stud or tape than to the properties of the metal–polymer laminate under investigation.

The symmetrical laminate approach has therefore been applied, in the first instance, to a relatively simple type of film, an unfilled grade of PET. Static fractographic studies of peel failure surfaces are reported elsewhere [2], and the present paper describes preliminary dynamic SEM studies which cast further light on the deformation and failure mechanisms involved.

2. Experimental details

2.1. Materials

The PET film used was 50 μm thick ICI "Melinex", type "0", an unfilled additive-free grade produced by biaxial drawing. Symmetrical PET–aluminium–PET laminates were produced by the thermal evaporation of aluminium on to two strips of PET while the latter were fed into a roll nip. A glow-discharge pretreatment of the PET film was used to promote bonding, and a typical thickness for the aluminium layer in the "sandwich" was 40 nm. Details of the lamination method [1, 3] and of the process parameters chosen for production of the present series of specimens [2] are given elsewhere.

Several methods of cutting the laminates for viewing "edge-on" in the SEM were tried: the most satisfactory method proved to be to lay the laminate on a hard surface (a clean ceramic tile) and to cut it carefully with a scalpel fitted with a fresh curved blade. This technique minimizes deformation around the cut and leaves a "clean" edge for SEM examination.

Present address: ICI plc, Agricultural Division, PO Box 1, Billingham, Cleveland, UK.
‡ *Present address*: BP Research Centre, Chertsey Road, Sunbury-on-Thames, Middlesex, UK.

0022–2461/86 $03.00 + .12

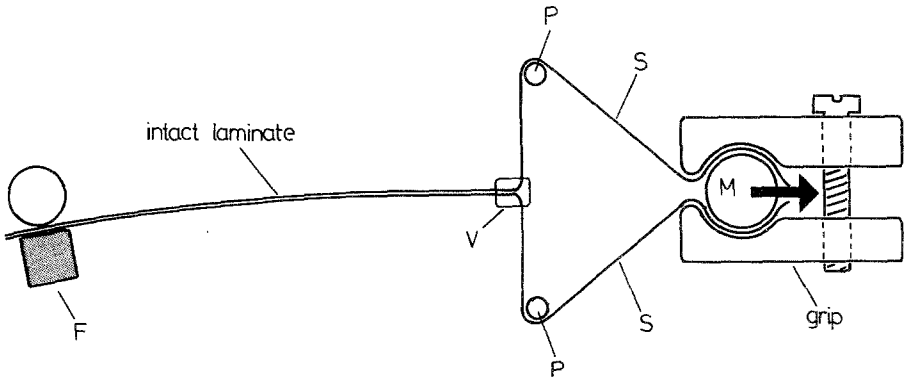

Figure 1 Schematic diagram of the specimen mounting geometry for dynamic SEM studies. Part of the laminate specimen is peeled by hand and the separated ends clipped to the moving mount, M. As the latter is displaced and peeling proceeds, the newly separated strips, S, are drawn round the fixed posts, P, so that the tip of the peel crack remains (nominally!) stationary with respect to the field of view, V. The intact part of the laminate is prevented from vibrating laterally by a small piece of open-cell plastic foam, F, glued to the baseplate next to a fixed mount. The arrow indicates the direction of displacement of the moving mount.

2.2. Dynamic peel testing

Previous dynamic observations of crack propagation in various polymeric systems have been made and experimental details given [4–6]. For continuous observation it is convenient to keep the tip of the peel crack stationary with respect to the field of view. For this purpose the arrangement illustrated in Fig. 1 was designed. A specimen of width 6 mm is cut from a laminate and peeled by hand for a few centimetres, so that the separated ends can be attached to the moving mounting boss, M, on the dynamic straining rig by means of a suitable grip. As peeling proceeds the two newly separated strips, S, are drawn from the peel crack tip around two small fixed posts, P, providing the required T-peel geometry. The intact portion of the specimen is, of course, free to move parallel to its length, but a small piece of open-cell plastic foam, F, serves to damp lateral vibration during peel.

Manual operation of the straining rig was found to be satisfactory. Measurements of peel force were performed on similar specimens using either an Instron (model 1026) displacement-controlled testing machine or a bench-top peel tester (Instrumentors Inc, Cleveland, Ohio, model SP-101A). Although these measurements were carried out at a higher strain rate (5 mm sec^{-1}) than the SEM experiments and in air, subsequent static SEM examination revealed no significant differences in the overall topography of the failure surface. Specimens similar to those discussed below exhibited peel forces of typically 300 N m^{-1}, i.e. peel energies of 600 J m^{-2} referred to the bonded area.

3. Observations of peel failure

Fig. 2 illustrates the profile of a typical laminate specimen during peel failure: the radius of curvature of each separated strip is about 1.3 mm, although this varies with local changes in bond strength and hence in applied force. Such a curvature implies a strain sufficient to fracture an aluminium film on or near either surface.

The similarity to a propagating crack is obvious, and in the vicinity of the propagating "peel crack" tip there will be, just as in the fracture of bulk materials, a plastic zone and an associated rapidly changing strain field related to the geometry of the specimen and to the mechanical properties of the laminate. Since the latter are anisotropic a theoretical analysis is difficult, but our method of specimen preparation allows the strain field to be visualized during a dynamic experiment. The thin sputtered metallic layer deposited on the cut edge of the specimen to minimize charging in the SEM is distorted near the crack tip. This leads to an interaction with the electron beam such that a brighter area appears around the tip. The video still in Fig. 3 shows such an area.

The velocity of crack propagation fluctuates during

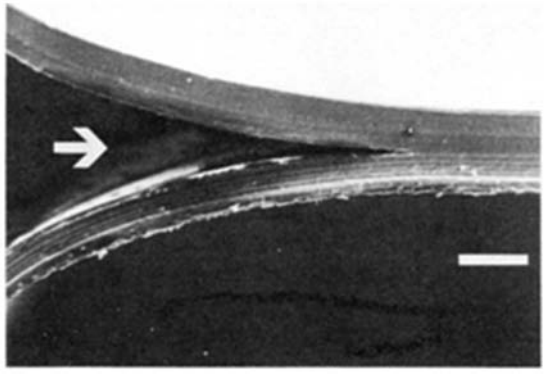

Figure 2 Profile of an aluminium–polyester–aluminium laminate during peel. Each polyester strip is 50 μm thick and 6 mm wide (perpendicular to the picture): the aluminium layer is of order 40 nm thick. Arrow denotes peel direction; scale bar 100 μm.

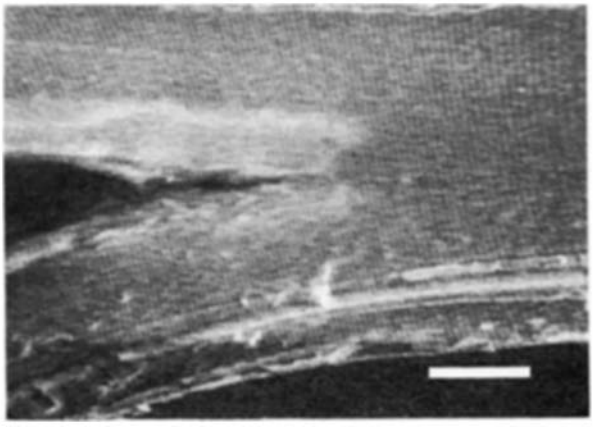

Figure 3 Video still of a laminate during peel, showing the visualization of the strain field around the crack tip. Scale bar 30 μm.

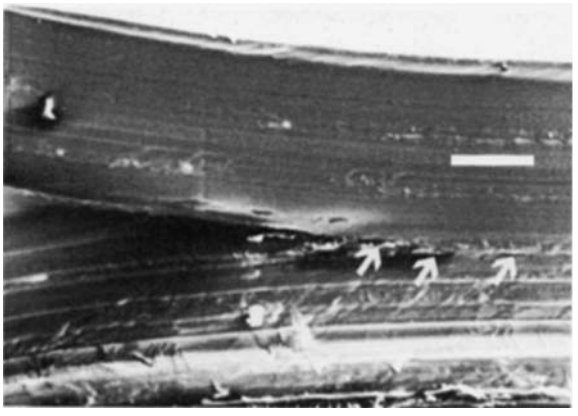

Figure 4 Microcracking: microcracks (arrowed) can be seen opening up several micrometres ahead of the main crack tip, while several others have formed on a different plane and have given rise to sub-surface cavities in the upper PET strip. Scale bar 30 μm.

the test. This is due in part to the variability of laminate strength, particularly where the inclusion of dust particles during fabrication leads to the formation of regions of low or zero metal–metal bond strength. A more significant reason for the fluctuation arises, however, from changes in the fracture plane during failure. Static SEM work [2] indicates that the peel crack propagates along different planes (i.e. at various distances from the true interface) in different regions of the failure surface, and suggests that crack advance may proceed by the linking-up of "microcracks" originally formed ahead of the main crack tip.

The dynamic SEM technique confirms the existence of such microcracks: Fig. 4 shows microcracking ahead of a propagating peel crack tip, together with a group of microcracks which formed at a slightly earlier stage but failed to coalesce with the main crack, remaining instead as cavities beneath the failure surface of the upper PET strip. The linking-up of a microcrack with the main fracture entails the deformation and breakage of the intervening material, and it is this which delays the peel propagation.

4. Mechanism of peel crack advance

The mechanism of crack propagation is seen in operation in the sequence of photographs in Fig. 5. In the interests of picture quality these are static photographs rather than video stills (i.e. the straining was halted before each photograph and the load slightly reduced to "stop" the deformation), so that they if anything underestimate the local strain near the crack tip. In other respects, however, the illustrations represent the process observed dynamically.

In Fig. 5a a microcrack has formed ahead of the main crack tip, and at a level a few micrometres above the plane of the latter. With further straining this microcrack has opened out to form a void: viewing the system on a rather broad scale the right-hand end of the microcrack is now looking like the new crack tip.

Meanwhile, the few micrometres thickness of polymer between the "old" and "new" portions of the crack has been bent out of the horizontal plane and is beginning to be stretched to form a ligament which will bridge the advancing crack. In three dimensions we will have a "web" of material extending parallel to the crack front: the degree of charging (indicated by the very bright areas in the photographs) demonstrates that fresh polymer, rather than aluminium, is being exposed.

In Fig. 5b the microcrack has been further enlarged, and the "web" has been stretched to form a highly extended ligament of PET bridging the crack. At the same time the microcrack has propagated forwards (this is easily seen by using some of the bright spots on the cut edge of the laminate as markers) and the presence of a new, smaller ligament nearer the effective crack tip reveals that the microcrack nucleation and void formation process has happened again, on a

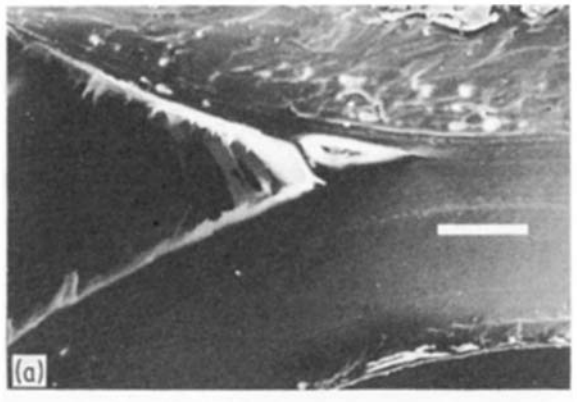

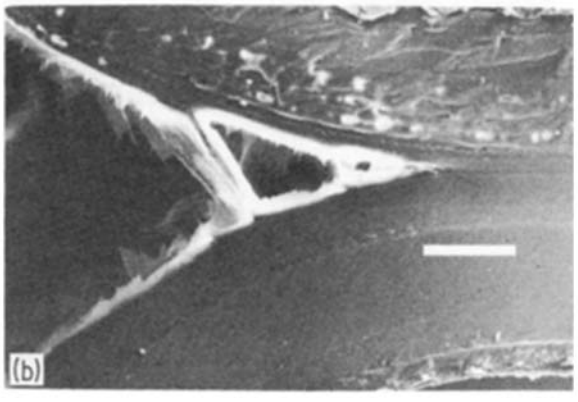

Figure 5 The proposed mechanism for crack advance seen in operation. (a) Opening of a microcrack ahead of the main crack tip and on a plane several micrometres above the latter; (b) stretching of the intervening material to form a ligament bridging the crack; (c) further ligament extension and forward crack growth: note the new microcrack forming near the current main crack tip. All scale bars 30 μm.

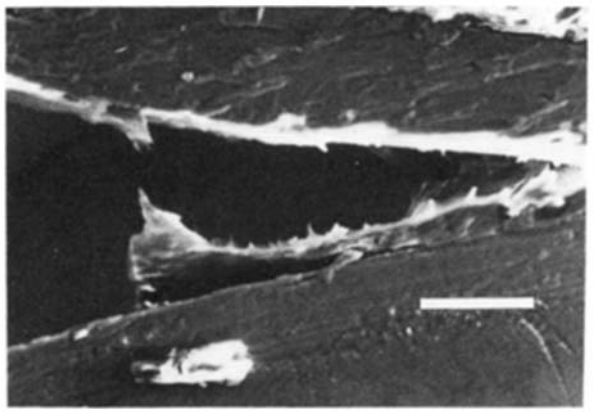

Figure 6 Crack branching: photograph taken just after breakage of load-bearing ligament. Scale bar 30 μm.

smaller scale this time. Slightly later still, in Fig. 5c, the earlier ligament is still intact but the smaller one has broken: a remnant of the latter can be seen on the lower crack face. Further forward growth has taken place, and a new microcrack has been formed ahead of and somewhat above the current main crack tip.

In all three micrographs, fine-scale tearing is visible on the newly created surfaces: tear ridges, reminiscent of the bulk yielding of polymers, or indeed of the ductile failure of metals, are being formed perpendicular to the peel direction.

Ligaments such as those illustrated in Fig. 5 will be load-bearing, and thus even after the advance microcrack has taken over the role of main crack tip, the original fracture need not stop at once: there may still be sufficient load transferred by the ligament to enable further propagation as a branch crack. Fig. 6 is a case in point: here the lower (original) fracture has extended for some tens of micrometres along a path up to 5 μm below the new main crack, continuing until the load-bearing ligament finally breaks.

Similarly, the load-bearing ligaments allow the possibility that, once a microcrack has opened up, the original crack path may again be favoured: Fig. 7 illustrates the consequent formation and breakage of a pair of ligaments, as though a surface layer of the lower PET film is being partially detached. This may occur repeatedly, as indicated by the lower part of Fig. 8.

5. Near-interfacial failure

We have concentrated so far on the mechanism of crack advance in well-bonded regions of the specimens. Since our specimens are prepared by a small-scale laboratory batch process, bond quality is inevitably rather variable within any one specimen. It is clear both from the changing rate of crack advance and from static SEM observation of the failure surfaces that well-bonded zones are interspersed with regions where failure has been energetically cheap and rapid. The route taken is so close to a true aluminium–PET interface that one side of the failed laminate exhibits a surface which, in the SEM, appears to be aluminium – a broken film of aluminium, because of the strain associated with the curvature of the peeling strip, but aluminium nonetheless. The broken film is illustrated in Fig. 9, where the darker "islands" represent aluminium which is less prone to charging than the exposed PET. They will not be entirely aluminium, however: their depth (somewhat less than 1 μm) is much greater than the thickness of the aluminium layer, while their upper surface may carry a thin coating of organic material, giving rise to an organic rather than a metallic surface signal in X-ray photoelectron spectroscopy [1].

6. Failure surface features

The possible modes of failure may be illustrated by examining the failure surfaces in a static SEM (in our case a Camscan S4 instrument) after sputter-coating with a thin layer of gold. Fig. 10 shows such a mating pair of failure surfaces. We can distinguish virtually featureless "haloes", around dust particles which have prevented successful metal–metal bonding; large areas of comparatively low relief representing low-energy, near-interfacial failure; and regions exhibiting massive ductile tearing and representing high-energy failure well within the bulk PET. The central part of Fig. 10a shows a large body of material torn away from the film in Fig. 10b. Here and on the right in Fig. 10a, the remains of ligaments can be identified, standing above the level of the surrounding fracture surface. These features, on a scale of tens of micrometres, we classify as "macroductile". Their formation, via microcracking ahead of the main crack tip (Fig. 5), often involves a step across the metallic layer: such a

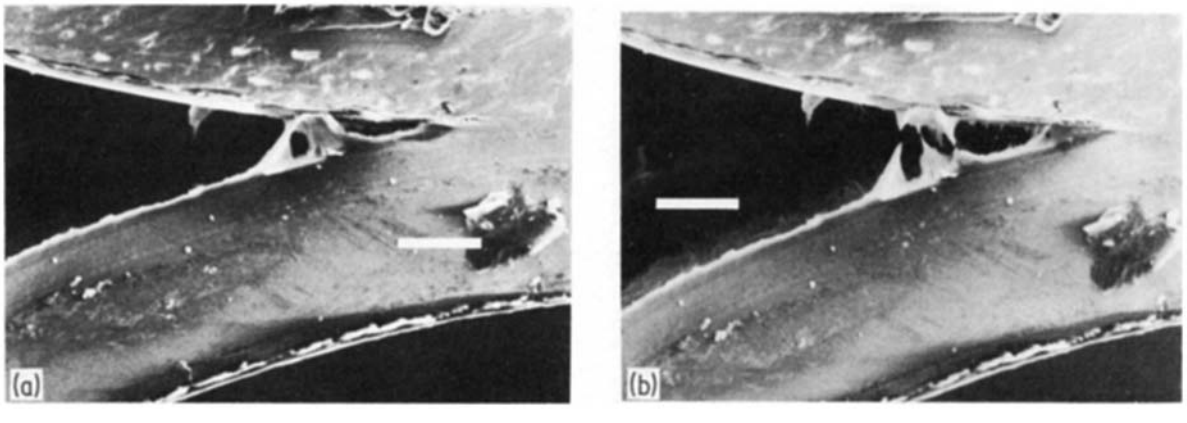

Figure 7 Partial removal of surface layers from the lower PET strip: (a) before breakage of ligaments; (b) after breakage. Scale bars 30 μm.

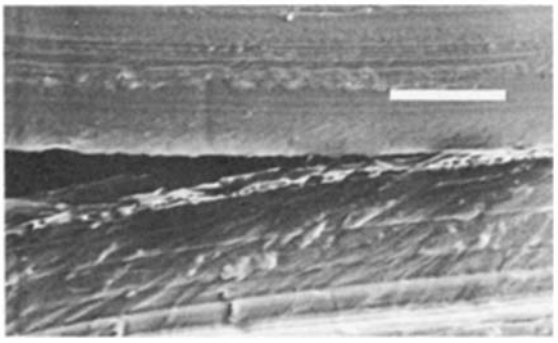

Figure 8 Repeated partial detachment of material from the film surface: some ligaments are still bridging the crack near its tip. Scale bar 30 μm.

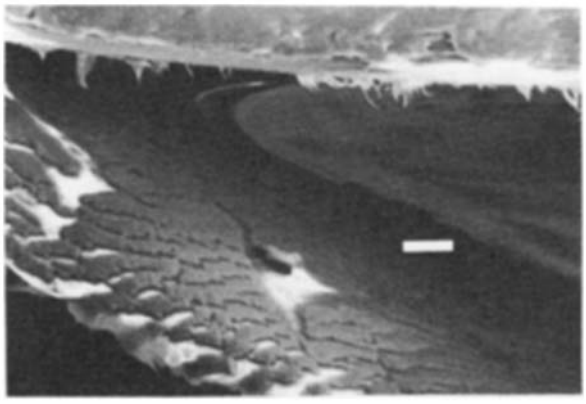

Figure 9 Fragmentation of the aluminium layer (together with some polymer). Darker "islands" represent aluminium-bearing material, lighter areas exposed PET. Peel direction left to right. Scale bar 10 μm.

ligament may thus itself be a miniature PET–aluminium–PET laminate.

Looking more closely at the central area of Figs. 10a and b, tear ridges corresponding to fine-scale tearing of the type noted in Fig. 5 can be distinguished. The extensive deformation associated with the tearing can be gauged qualitatively from Fig. 11, a close-up of the central region of Fig. 10a: the tear ridges are typically of the order of 1 μm apart, and we will classify this type of deformation as "microductile". Deformation on this scale, though less pronounced, is apparent on the lower-relief zones, suggesting that significant energy-dissipative mechanisms operate even when fracture follows a path close to the aluminium layer. In contrast to macroductile features, microductile behaviour seems to involve only the PET and not the aluminium layer.

Optical examination reveals that the aluminium is distributed over both failure surfaces, since fracture can propagate on either side of the metallic layer. In the featureless "haloes" aluminium is observed on both failure surfaces; elsewhere, it is entirely on one failure surface or the other – although the failure path alternates so frequently from side to side of the metal as to leave metallic "patches" only a few tens of micrometres in extent.

Examination of the edge of the failure surface enables us to correlate the "surface" and "edge-on" views of the peeled specimen: Fig. 12, taken from the aluminium-bearing side of the failed laminate, shows a sub-surface cavity (arrowed) due to a microcrack which has not coalesced with the main crack, together with (on the right of the picture) a large "tongue" of PET, partially detached from the underlying film by a crack branching process similar to that of Fig. 6. During peel, this material will have acted as a load-bearing ligament until breakage.

On a smaller scale, the microductile tear ridges also provide load-bearing elements bridging the crack tip. If we examine the tip of the branch crack in Fig. 12 at higher magnification (Fig. 13) we see a series of tear ridges, one of which (at the extreme right in the photograph) is still bridging the crack tip. This behaviour in the vicinity of the tip suggests an analogy with crack-tip crazing: though the scale of the features seen here is considerably greater than that of craze fibrils, there is an important feature in common in that stress can be supported behind the crack tip itself – influencing the stress distribution and hence the local crack profile.

7. Energy dissipation and the fracture path

The most obvious contribution to the energy of a fracture process, the creation of new surfaces with their associated energy, will make only a small contribution to the failure energy. If the new surfaces were flat the PET surface energy contribution would be of order 0.1 J m^{-2}: they are, of course, not flat, but even

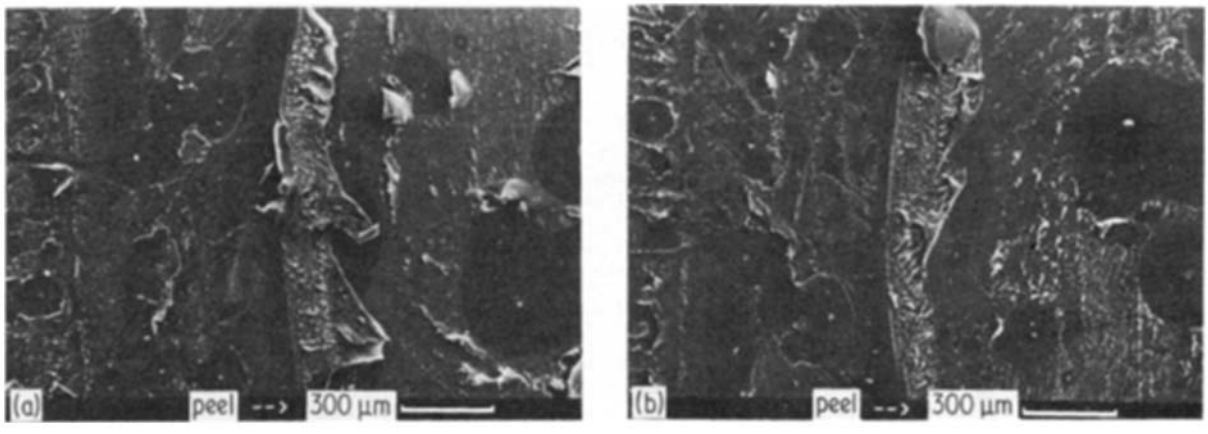

Figure 10 Static SEM fractographs of a mating pair of peel failure surfaces. Peel direction left to right.

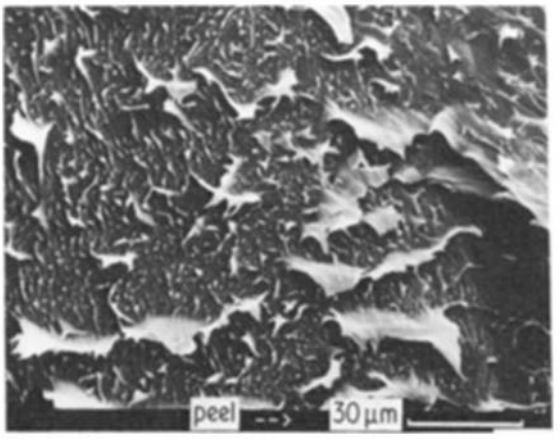

Figure 11 Close-up of a central part of Fig. 10a, showing extensive microductile deformation leading to the formation of tear ridges.

a hundred-fold increase due to fracture surface relief would account for barely 1% of the typical 600 J m^{-2} failure energy. The measured values will thus be determined overwhelmingly by the energy-dissipative deformation processes accompanying peel fracture. Extensive plasticity in the surface regions of the polyester films is the combined result of macroductile deformation processes – ligament formation, extension and fracture associated with changes in the failure plane – and the finer scale microductile tearing which takes place in the vicinity of the peel crack tip. To predict the failure energy on theoretical grounds would require a detailed knowledge of the mechanical situation near the tip, but an approximate calculation will indicate whether the measured values are reasonable in the light of observation. Manufacturer's data [7] (averaging between machine and transverse directions) give the strain to fracture of the PET film in uniaxial geometry as about 118% and the yield stress in the film plane as 106 MPa: making a first-order rigid-plastic assumption the energy to failure per unit volume should therefore be about 125 MJ m^{-3}. If we apply this value to the PET film laminates, it would correspond to extensive deformation of the two polyester strips to an average depth of 2.4 μm.

It is significant that this estimate of the likely thickness of the deformed layer is of the same order as the

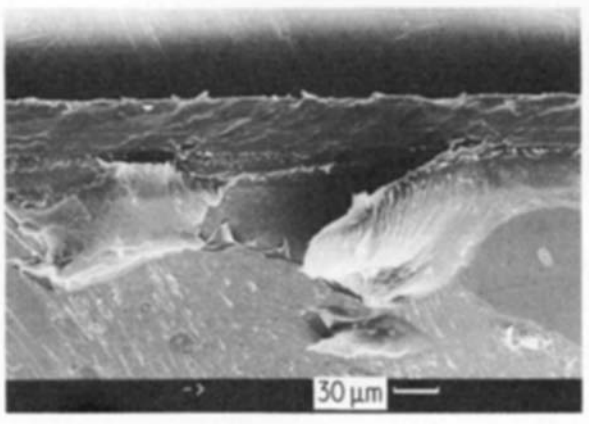

F
(lower) and part of the cut edge as examined in the dynamic SEM (upper). Arrow indicates a cavity beneath the failure surface: peel direction left to right.

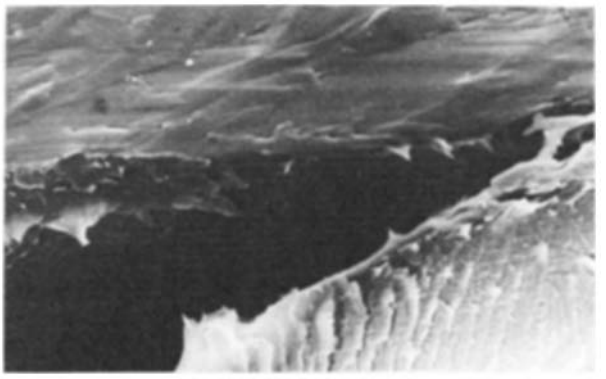

Figure 13 Close-up of part of Fig. 11, showing microductile tearing on the faces of the branch crack.

few micrometres within which the local fracture path is seen to deviate from the metal–polymer interface. However, before exploring the implications of this agreement further, we must consider whether there are other contributions to the energy of fracture which are not associated with plasticity near the crack tip. Gross yielding of the polyester strip can be ruled out, since for the 50 μm polyester film used in these experiments the applied stress does not exceed 6% of the reported tensile yield stress of the polymer [7]. Another possibility is that the bending of the polymer strips in the T-peel test might be sufficient to induce plastic deformation near the surfaces. The radius of curvature in Fig. 2 is about 1.3 mm, which on the basis of simple beam theory using the published Young's modulus of 5.1 GPa [7] leads to an estimate for the stress at the curved surfaces of 98 MPa. This is comparable to the yield stress, but the absence of permanent bending in the polyester strips after testing indicates that there is no post-fracture plastic deformation on a scale which would significantly influence the measured values of peel energy.

The experimental evidence thus supports the view that the dominant contribution to the peel energy arises from the creation and growth of microcracks in the vicinity of the main crack tip, and the consequent formation, deformation and fracture of thin ligaments which span the fracture path as a consequence of the "jumping" of the crack between various parallel failure planes within a few micrometers of the polymer–metal interfaces.

There remains the question as to why the fracture ıth, while not following the metal–polymer interface, :hibits little tendency to deviate from it by more than few micrometres. It would appear that although ıere are many competitive parallel failure paths, they 'e concentrated near to the bonded surfaces. 'hether this is the result of a variation in structure ıd hence properties through the thickness of the ɔlyester film, or whether it is a consequence of the ress distribution associated with the propagating ɔel failure, is not clear.

The most likely structural influence on the preferred ilure path would arise from variations in quality of olecular orientation or in degree of crystallinity with depth below the polymer surface. Either factor might be associated with a greater tendency to delaminate within the surface regions of the film, which would

effectively confine the propagating fracture to the central part of the laminate. Neither of these aspects of structure has received much attention in the open literature, at least as far as through-thickness variations are concerned, but further studies are in progress.

Alternatively, the stress distribution might affect the locus of fracture in one of several ways. We have already noted that the curvature of each polyester strip is sufficient to induce near the surface an elastic stress comparable to the yield stress, and this will come into play as soon as the strip starts to bend, i.e. near to the peel crack tip. Depending upon the yielding mechanism and criterion, the stress normal to the film plane required to give rise to plastic flow may be reduced by the presence of a high tensile stress in the peel direction. The initiation of plasticity would thus become more difficult with depth. Another approach is in line with the interpretation advanced by Bascom *et al.* [8] of the observation that fracture of the bond between epoxy resin and bulk aluminium often proceeds along a path which is cohesive within the epoxy resin but close to the interface. They show that in their scarf-joint geometry the crack is "mechanically focused" towards the interface, and suggest that it will not approach close to the interface with the much stiffer aluminium than is consistent with a plastic zone lying entirely within the polymer. Finally, consideration must be given to the possibility of the stress field in the polymer immediately adjacent to the metal being modified by stresses associated with the development of the interfacial oxide layer following vacuum deposition of the aluminium.

9. Conclusions

Dynamic studies of laminate peel failure underline the importance of local plastic deformation processes in the vicinity of the "peel crack" tip. The SEM evidence points to failure propagation along a variety of planes in different regions of the specimen, but falling into one of three broad categories:

1. slow, high-energy failure along any of a number of planes within either strip of polyester film, typically several micrometres from the PET–aluminium interface;
2. failure at or near one of the PET–aluminium interfaces;
3. apparent laminate failure leaving a coating of aluminium on both fracture surfaces – this is a significant contribution only in regions where the two PET strips, each carrying a newly deposited aluminium layer, have failed to laminate together successfully during fabrication [1].

Failure of type 1 proceeds by a mechanism involving advance microcracking, followed by ligament formation, extension and breakage associated with changes in the failure plane: the resulting fracture surface displays both macroductile relief (on a scale of tens of micrometres) and microductile tearing (on a scale of order 1 μm). Failure of type 2 exhibits evidence of plastic deformation, but the deformation (again on a microductile scale) is less pronounced. The macroductile ligament formation, and on a smaller scale the creation of microductile tear ridges, imply some load-bearing ability behind the advancing crack tip.

Deformation is highly concentrated near the surface of the PET film. The measured failure energy is consistent with a mean "deformation depth" of order 2 to 3 μm over each of the failure surfaces. Bending stresses near the interface are of a magnitude comparable to the uniaxial yield stress, and may help to induce plastic flow in this region.

The propensity of the peel fracture to propagate along a path several micrometres from the aluminium layer is consistent with the possible structural and mechanical factors which may affect the choice of failure path. The absence of information on through-thickness variations in film properties, however, precludes a quantitative assessment of the relative roles of these factors.

Acknowledgements

The authors thank Philip Lamb for preparing the laminates, and Dr W. C. Nixon for his continuing interest in the subject. This work forms part of a programme of studies in Cambridge University Engineering Department on the dynamic fracture of materials, supported in part by the SERC. D. J. B. is grateful to ICI plc, Petrochemicals and Plastics Division, for financial support and for the supply of the PET film. D. G. G. acknowledges the financial support of the SERC.

References

1. N. J. GIBBINS and A. H. WINDLE, *Mater. Sci. Technol.* **1** (1985) 263.
2. D. J. BROWN, P. LAMB and A. H. WINDLE, to be published.
3. N. J. GIBBINS and A. H. WINDLE, *J. Mater. Sci.* in press.
4. S. WILLIAMS, PhD thesis, Cambridge University Engineering Department (1983).
5. T. H. MAO, P. W. R. BEAUMONT and W. C. NIXON, *J. Mater. Sci. Lett.* **2** (1983) 613.
6. D. G. GILBERT, P. W. R. BEAUMONT and W. C. NIXON, *ibid.* **3** (1984) 961.
7. Industry Note MX200, "'Melinex' Properties", ICI plc, Petrochemicals and Plastics Division, Middlesbrough, UK.
8. W. D. BASCOM, C. O. TIMMONS and R. L. JONES, *J. Mater. Sci.* **10** (1975) 1037.

Received 14 February
and accepted 13 March 1985